

Article

# Experimental Investigation of Primary De-NO<sub>x</sub> Methods Application Effects on NO<sub>x</sub> and CO Emissions from a Small-Scale Furnace

Ladislav Lukáč <sup>1,\*</sup>, Miroslav Rimár <sup>2</sup>, Miroslav Variny <sup>3</sup>, Ján Kizek <sup>2</sup>, Peter Lukáč <sup>4</sup>, Gustáv Jablonský <sup>1</sup>, Ján Janošovský <sup>3</sup> and Marcel Fedák <sup>2</sup>

<sup>1</sup> Department of Thermal Technology and Gas Industry, Institute of Metallurgy, Faculty of Materials, Metallurgy and Recycling, Technical University of Kosice, Letná 9, 042 00 Košice, Slovakia; gustav.jablonsky@tuke.sk

<sup>2</sup> Department of Process Technique, Faculty of Manufacturing Technologies of the TU of Kosice with a Seat in Prešov, Technical University of Kosice, Štúrova 31, 080 01 Prešov, Slovakia; miroslav.rimar@tuke.sk (M.R.); jan.kizek@tuke.sk (J.K.); marcel.fedak@tuke.sk (M.F.)

<sup>3</sup> Department of Chemical and Biochemical Engineering, Faculty of Chemical and Food Technology, Slovak University of Technology, Radlinského 9, 812 37 Bratislava, Slovakia; miroslav.variny@stuba.sk (M.V.); jan.janosovsky@stuba.sk (J.J.)

<sup>4</sup> Department of Power Engineering, Institute of Power and Process Engineering, Faculty of Mechanical Engineering, Technical University of Košice, Letná 9, 042 00 Košice, Slovakia; peter.lukac@tuke.sk

\* Correspondence: ladislav.lukac@tuke.sk

Received: 30 June 2020; Accepted: 2 August 2020; Published: 5 August 2020



**Abstract:** Nitrogen oxides (NO<sub>x</sub>) from combustion contribute significantly to atmospheric pollution. An experimental setup was employed to investigate the application of three primary denitrification methods, i.e., reburning (staged combustion), overfiring air (OFA), and flue-gas recirculation (FGR), individually and in combination, combusting natural gas (NG) and propane–butane gas (PBG). Fuel heat inputs of 16 and 18 kW and air excess coefficients of 1.1 and 1.2, respectively, were tested. The highest individual denitrification efficiency of up to 74% was obtained for FGR, followed by reburning and OFA. A denitrification efficiency between 8.9% (reburning + OFA) and 72% (reburning + OFA + FGR) with NG combustion was observed. Using a 20% FGR rate yielded denitrification efficiency of 74% for NG and 65% for PBG and also led to a significant decrease in carbon monoxide (CO) emissions, so this can be recommended as the most efficient denitrification and de-CO method in small-scale furnaces. Reburning alone led to a sharp, more than 12-fold increase in CO emissions compared to the amount without any other method application. The presented results and the difference between our experimental data and the literature data acquired in some other studies indicate the need for further research.

**Keywords:** nitrogen oxides; reburning; flue-gas recirculation; furnace; combustion

## 1. Introduction

The use of primary energy sources (fuels) burdens the environment and impacts human health, both in the fuel mining and processing phases [1] as well as in the conversion processes to heat and power [2] or to mechanical energy in transportation systems [3]. Combustion of fuels yields, besides heat, harmful substances emitted into the atmosphere, such as fly-ash, particulate matter, carbon, sulphur, and nitrogen oxides as well as light and heavy metals (often radioactive), especially in liquid and solid fuel combustion. Nitrogen oxides (especially NO and NO<sub>2</sub>) and their formation and reduction strategies, therefore, play an important role in the protection of the atmosphere [4].

NO<sub>x</sub> formation during combustion is influenced by several parameters. The most important ones include combustion temperature, fuel nitrogen content and fuel composition [5,6], air excess coefficient [7] and air staging [7,8], combustion process reaction pathways [9], hydrodynamics, burner design [10] and load [5,7], and flue gas residence time [11]. Numerical studies using dedicated software enable their synergies to be assessed [12–15].

Oxycombustion is a widely studied means of combustion process energy efficiency improvement nowadays but with an ambiguous effect on NO<sub>x</sub> formation [16–18]. A recent review by Liu et al., 2019 [19], surveyed the most important experimental research in the field of oxycombustion, concluding that NO<sub>x</sub> formation was case-sensitive, strongly dependent on system design and operation specificities, and no general conclusion could be drawn on the impact of oxygen enrichment on NO<sub>x</sub> formation.

The development and application of advanced flue gas denitrification methods have facilitated meeting the nitrogen oxide limit concentrations, which are steadily becoming more stringent [20]. Denitrification methods can be classified into primary and secondary ones [4,21]. Primary de-NO<sub>x</sub> methods are based on nitrogen formation suppression directly during fuel combustion through the creation of a reduction zone, which lowers the flame temperature [22]. Secondary de-NO<sub>x</sub> methods are based on nitrogen oxide reduction or scavenging from the flue gas downstream of combustion processes [23,24].

Primary methods include overfire air (OFA) [10,11,25–28], reburning [12,29–37], flue-gas recirculation (FGR) [13,23,38–41], and their combinations [14,42–45]. They are cheaper than the secondary ones, however the thermal efficiency of combustion aggregate decreases as a result of combustion temperature lowering, and there is a subsequent increase in unburnt carbon content in ash and fly-ash. OFA is based on substoichiometric ( $m = 0.7$  to  $0.8$ ) fuel combustion with air [25]. The resulting reduction atmosphere suppresses nitrogen oxide formation. Previous studies [10,27,28] confirm that staged air introduction can help in reducing NO<sub>x</sub> emissions from combustion but can negatively impact the energy performance of the combustion process. The “reburning” method includes the creation of a zone in the combustion chamber with a lack of oxygen, which in turn leads to nitrogen oxide reduction [12,29]. Low-quality gaseous or solid fuel or waste fuels can be used for this purpose [30]. Primary fuel is combusted with a substantial air excess coefficient, which decreases flame temperature and suppresses NO<sub>x</sub> formation [31]. Optimal means of reburning integration with other denitrification methods for further improvement in NO<sub>x</sub> emissions reduction were proposed in [14,42]. Flue-gas recirculation (FGR) is one of the simplest and cheapest denitrification methods. It is based on returning part of the obtained flue gas back to the combustion zone. Internal recirculation is achieved in modified burners, resulting in combustion air and flue gas mixing [38,39]. External recirculation is characterized by returning part of the partly cooled flue gas into the space above the burners [15,40]. Flue-gas recirculation is a cheap denitrification method, which is often used to assist other methods in achieving greater denitrification.

Analyzed studies suggest that the synergic effect of simultaneous application of multiple primary denitrification methods varies significantly with the fuels combusted as well as with combustor operation and design. Effects on the emissions of other pollutants, such as carbon monoxide, are to be considered along with NO<sub>x</sub> emissions to truly prove the beneficial environmental impact of specific denitrification methods. Comprehensive information on their application can be found in a few recently published studies [35,44] with significant differences in their findings. So the key question to be answered with the intention of contributing significantly to environmental protection is: which individual method and which combination of methods would serve as the best for reducing nitrogen oxide emissions while also preventing an increase in other gaseous pollutants? The present experimental study addresses this question by investigating the application and resulting denitrification efficiency of several primary denitrification methods and their combinations and evaluating their impact on carbon monoxide emissions as well. The methods and combinations applied were:

1. OFA
2. Reburning
3. FGR
4. OFA + reburning
5. OFA + reburning + FGR

Natural gas and propane–butane gas served as widely available gaseous fuels. In this way, problems related to particle sizes and their distribution, their porosities, moisture content, and many others, which must be considered when testing solid fuels, did not arise. Carbon monoxide is a common product of incomplete combustion, thus studying changes in its emission levels along with the application of various denitrification methods can be considered representative enough to assess those of other relevant greenhouse gases as well.

## 2. Materials and Methods

### 2.1. Experimental Setup

The experimental setup used for denitrification efficiency estimation of individual nitrogen oxide emissions reduction methods and their combination is shown in Figure 1. The following parameters were adjusted in the FGR method: recirculation rate, combustion air excess, and fuel flow rate. The reburning method used an adjustable reburning fuel flow rate. Denitrification efficiency in all three primary methods applied individually and in combination was evaluated at a constant fuel heat input.

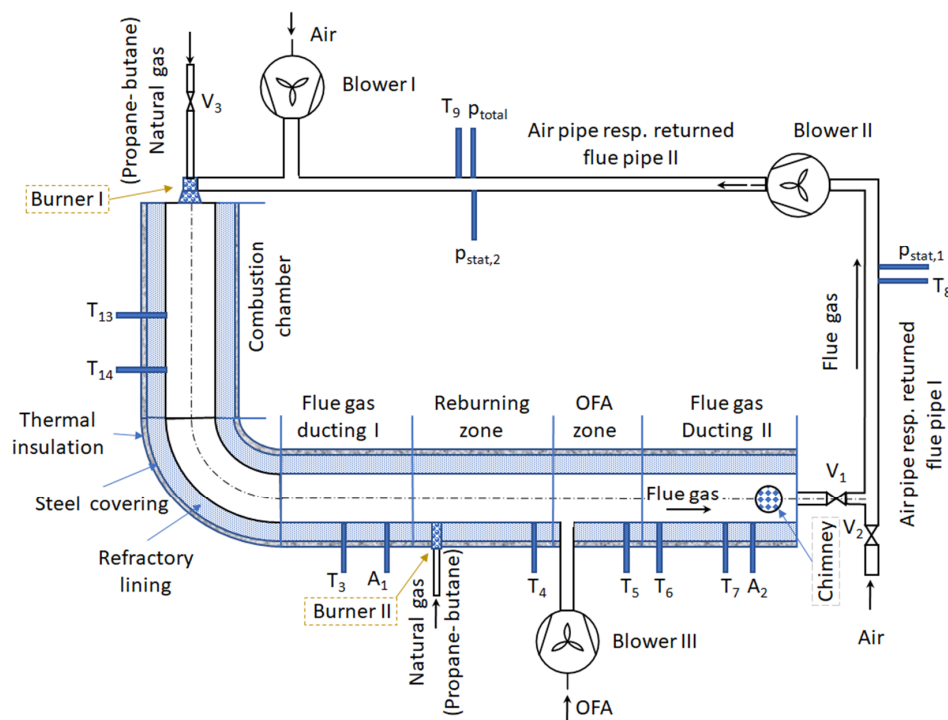


**Figure 1.** Experimental setup scheme with main equipment dimensions listed in mm. Legend: T—thermocouple, A—analyzer, V—throttle valve,  $p_{stat}$ —static pressure,  $p_{total}$ —total pressure, OFA— overfire air.

The experimental setup comprised the following: combustion chamber, flue-gas duct, stack, and three fans. The main burner combusting premixed primary fuel with air (primary air in the OFA application) was located at the front of the combustion chamber. Two Pt-RhPt thermocouples (T13, T14)

were located in the combustion chamber. Reburning fuel could be introduced into the central part of the flue-gas duct, and the reburning zone was followed by OFA entry and the afterburning zone.

Temperature in the flue-gas duct was measured by means of five Cr-Al thermocouples (T3 to T7). Two flue-gas analyzers (A1 and A2) served for flue-gas composition estimation in the duct and at the flue gas to stack discharge point. Supplementary burners were operated at the top of the stack to reduce CO emissions into the environment. Fuel flow rates were regulated with throttling valves. Natural gas was provided from the distribution network and propane–butane gas was supplied from gas cylinders. The composition of NG and PBG is provided in Tables 1 and 2, respectively.

**Table 1.** Composition of natural gas (NG) in % vol.

| CH <sub>4</sub> | C <sub>2</sub> H <sub>6</sub> | C <sub>3</sub> H <sub>8</sub> | C <sub>4</sub> H <sub>10</sub> | C <sub>5</sub> H <sub>12</sub> | CO <sub>2</sub> | N <sub>2</sub> |
|-----------------|-------------------------------|-------------------------------|--------------------------------|--------------------------------|-----------------|----------------|
| 98.04%          | 0.77%                         | 0.26%                         | 0.08%                          | 0.02%                          | 0.06%           | 0.77%          |

**Table 2.** Composition and properties of propane–butane gas (PBG).

| Propane–Butane                 | Density in the Liquid Phase (kg/dm <sup>3</sup> ) | Density in the Gas Phase (kg/m <sup>3</sup> ) | Calorific Value (Lower Heating Value) (MJ/m <sup>3</sup> ) | Composition (% vol.) |
|--------------------------------|---|---|--|----------------------|
| C <sub>3</sub> H <sub>8</sub>  | 0.508   | 2.019   | 92.97  | 40                   |
| C <sub>4</sub> H <sub>10</sub> | 0.585   | 2.59  | 123.74   | 60                   |

Thermocouple T3 and analyzer A1 were located in the first part of the duct, enabling us to monitor flue-gas temperature and composition before reburning and the OFA zone. The other four thermocouples were located downstream: T4 at the end of the reburning zone, T5 at the afterburning zone end, and T6 and T7 in the second part of the duct.

Positions of individual thermocouples and their distance from the burner, as shown in Figure 1, are specified in Table 3.

**Table 3.** Distance of individual thermocouples from burner outflow.

| Thermocouple | T13  | T14  | T3   | T4  | T5   | T6  | T7  |
|--------------|------|------|------|-----|------|-----|-----|
| Distance (m) | 0.25 | 0.35 | 0.95 | 1.7 | 1.95 | 2.0 | 2.1 |

The following gas meters were used for fuel flow rate estimation:

Primary fuel: type G 4 BK,  $Q_{\max} = 6 \text{ m}^3/\text{h}$ ,  $Q_{\min} = 0.016 \text{ m}^3/\text{h}$ ,  $V = 1.2 \text{ dm}^3$ ,  $p_{\max} = 20 \text{ kPa}$ , 1 imp 0.01 m<sup>3</sup>,

Reburning fuel: type G 1.6 BK,  $Q_{\max} = 2.5 \text{ m}^3/\text{h}$ ,  $Q_{\min} = 0.016 \text{ m}^3/\text{h}$ ,  $V = 1.2 \text{ dm}^3$ ,  $p_{\max} = 20 \text{ kPa}$ , 1 imp 0.01 m<sup>3</sup>.

Testo 350 XL (A2) and Testo 325 (A1) analyzers were employed for the flue-gas composition analysis. Appendix A contains detailed information about NO<sub>x</sub> and CO measurement methods and measurement errors of both analyzers.

## 2.2. Primary Denitrification Methods Application

Measurements with NG used both as main and reburning fuel were conducted under steady air excess coefficient conditions ( $m = 1.1$  or  $1.2$ ) and under steady fuel thermal inputs of 16 or 18 kW, respectively.

NO<sub>x</sub> emissions were measured first without any de-NO<sub>x</sub> method application, followed by application of individual methods and subsequently their combinations.

Emissions of nitrogen oxides and carbon monoxide as well as flue-gas temperature measurements were performed for various natural gas total heat inputs under various process modifications. An overview of performed experiments with individual methods and their combinations is provided in Table 4.

**Table 4.** Primary methods applied individually and in combination. Legend: FGR—flue-gas recirculation.

| Ratio  | Combustion without/with Primary Denitrification Method Applied Individually |                 |                       |     |
|--|---|-----------------|-----------------------|-----|
|  | Without   | FGR             | Reburning             | OFA |
| 10, 15, 20%<br>10, 15, 20, 25%   |   |                 |                       |     |
| Combustion with Primary Denitrification Methods Applied in Combination |   |                 |                       |     |
| Combination  |   |                 | 10, 15, 20% Reburning | OFA |
| Combination  |   | 10, 15, 20% FGR | 10% Reburning         | OFA |

Measurements with PBG combusted were conducted under steady air excess coefficient conditions ( $m = 1.1$  or  $1.2$ ) and under steady fuel thermal inputs of 16 to 22 kW, respectively. Combustion without any primary method application was compared with flue-gas recirculation rate of 10 to 20% in measurements.

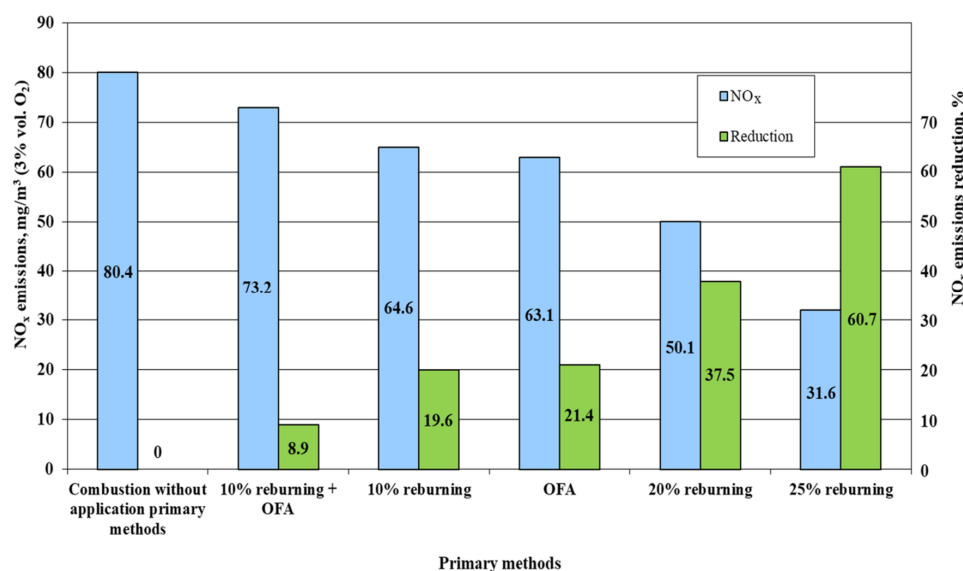
A detailed description of performed measurements is provided in Appendix B.

### 3. Results

#### 3.1. Natural Gas (NG) Combustion Experiments

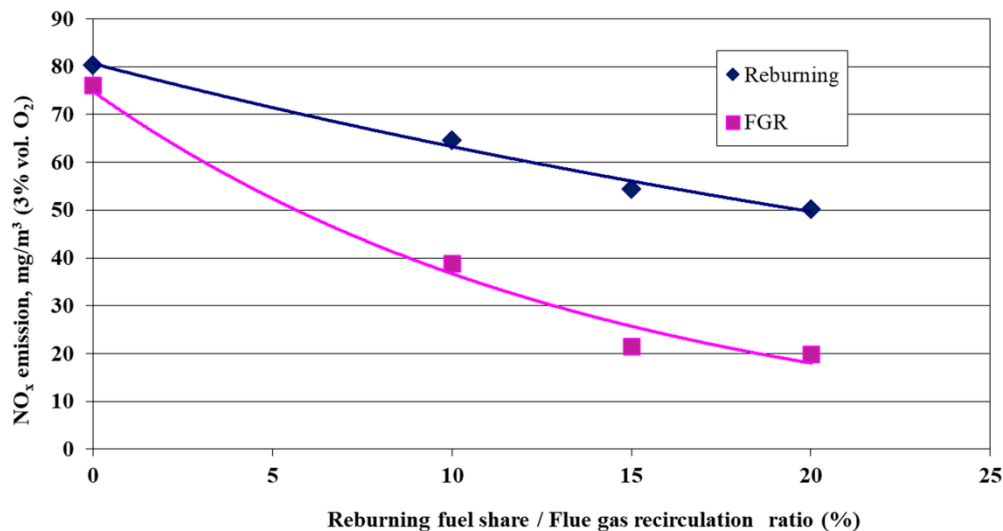
This section presents the results of applying primary de- $\text{NO}_x$  methods to a natural gas-fired system. Denitrification efficiency of flue-gas recirculation, reburning, overfire air use, and combinations of these were evaluated at natural gas thermal inputs of  $Q = 1.5$  and  $1.8 \text{ m}^3/\text{h}$  and air excess coefficients of  $m = 1.1$  and  $1.2$ , respectively.

Figure 2 depicts the measured nitrogen oxide emissions and denitrification efficiency of individual primary methods and their combinations at  $Q = 1.5 \text{ m}^3/\text{h}$  and  $m = 1.1$ . Reburning proved to be an efficient primary method; with a rising reburning ratio from 10 to 25%, the denitrification efficiency rose from 9 to over 60%. Overfire air use, whether applied separately or in combination with reburning, did not lead to a significant nitrogen emissions reduction.



**Figure 2.** Nitrogen oxide emissions (expressed in  $\text{mg}/\text{m}^3$  at 3% vol. oxygen in dry flue gas under normal temperature and pressure) and their reduction after the application of reburning and overfire air methods at total fuel input  $Q = 1.5 \text{ m}^3/\text{h}$  and air excess coefficient  $m = 1.1$ .

The effects of flue-gas recirculation on nitrogen emissions and its comparison with reburning application at  $Q = 1.5 \text{ m}^3/\text{h}$  and  $m = 1.1$  are shown in Figure 3. Flue-gas recirculation halved the  $\text{NO}_x$  emissions even at 10% recirculation, and the final  $\text{NO}_x$  emissions at 20% flue-gas recirculation dropped to roughly  $20 \text{ mg}/\text{m}^3$ , representing denitrification efficiency of almost 75%. A further increase in flue-gas recirculation was hindered by a significant increase in CO emissions, leading us to conclude that flue-gas recirculation of 20% is the upper limit for feasible combustor operation. Comparison with reburning shows that flue-gas recirculation is a more efficient  $\text{NO}_x$  emissions reduction method, as it reduced them by half at a reburning ratio of over 20% (compare Figures 2 and 3), while 25% represents the upper limit of commonly applied reburning ratios.



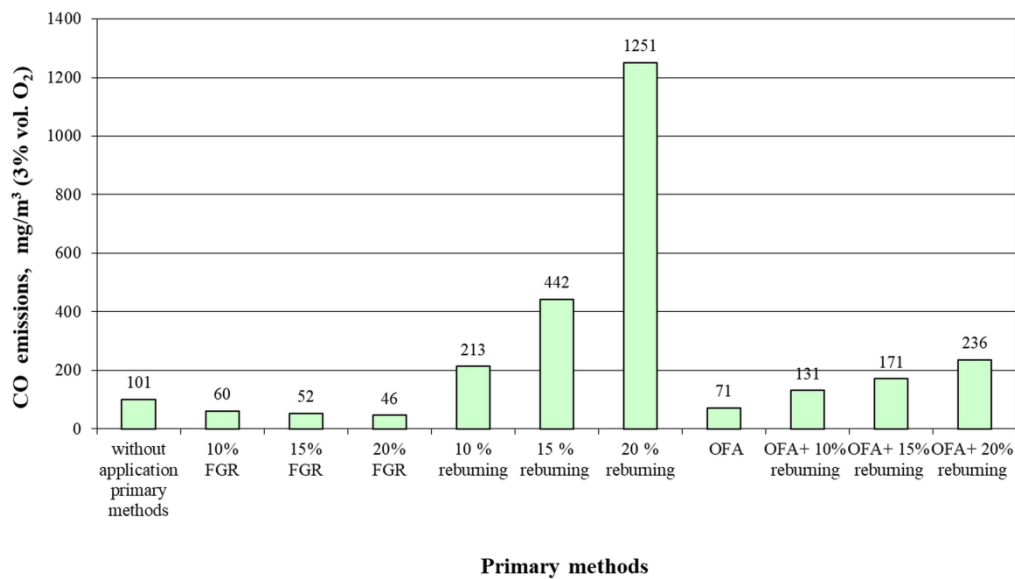
**Figure 3.** Flue-gas recirculation and reburning methods: denitrification efficiency comparison at total fuel input  $Q = 1.5 \text{ m}^3/\text{h}$  and air excess coefficient  $m = 1.1$ .

The nitrogen oxide reduction values shown in Figure 2 were calculated as relative nitrogen oxide emission differences resulting from measured nitrogen oxide emissions after primary methods application compared to those measured without any denitrification method applied, as follows:

$$R = \frac{(C_{WAPM} - C_{APM})}{C_{WAPM}} \cdot 100 (\%) \quad (1)$$

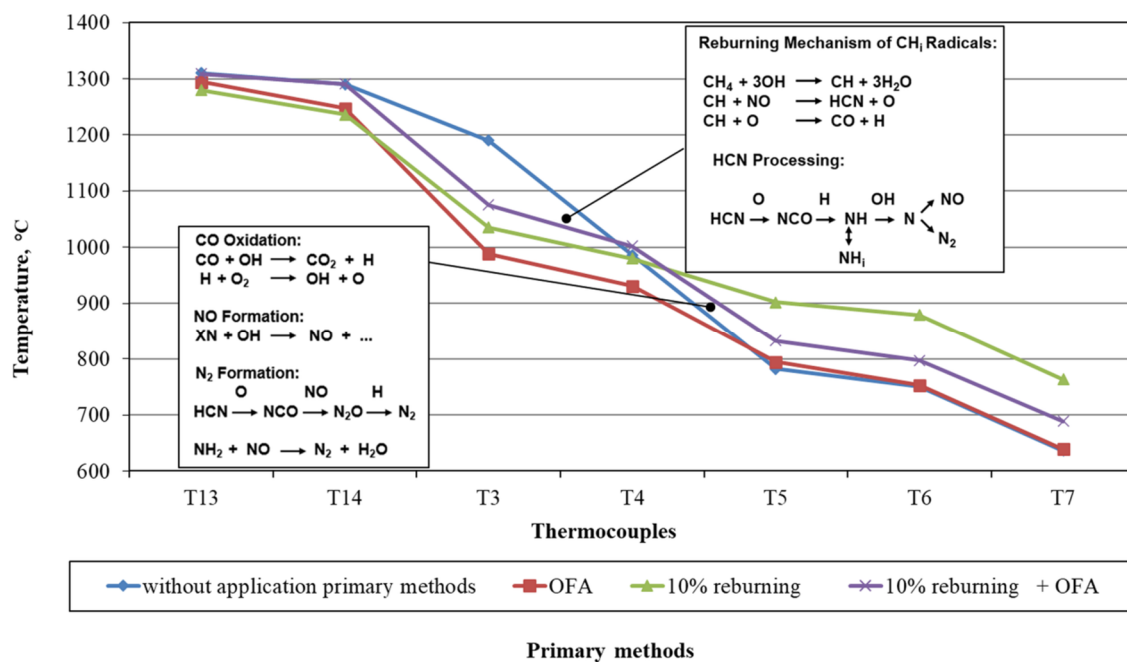
where  $R$  refers to emissions reduction (%),  $C_{WAPM}$  stands for nitrogen oxide emissions without application of primary methods, and  $C_{APM}$  represents emissions with application of primary methods.

Figure 4 presents the trends in carbon monoxide content in flue gas with the application of individual primary methods and their combinations. Flue-gas recirculation applied alone helped in decreasing CO emissions, compared to the situation without the application of any de- $\text{NO}_x$  method. Therefore, it can be concluded that the FGR method was able to significantly reduce both  $\text{NO}_x$  and CO emissions (see Figure 3 for comparison) and could thus be considered as a very promising method when striving towards reduction of combustion processes' environmental impact. All other de- $\text{NO}_x$  methods and their combinations resulted in increased CO emissions by around  $30 \text{ mg}/\text{m}^3$  (OFA + 10% reburning) to over  $1100 \text{ mg}/\text{m}^3$  (20% reburning). Reburning itself proved to be a less effective de- $\text{NO}_x$  method than FGR (see Figure 3), yielding substantially higher CO emissions than FGR. Therefore, the application of reburning alone does not appear sensible. Its combination with overfire air, however, reduced the  $\text{NO}_x$  emissions significantly (see Figure 2) and helped approach the emission limit for CO ( $200 \text{ mg}/\text{m}^3$ ). This results from the fact that overfire air introduction leads to oxidation of a major portion of the carbon monoxide formed in the reburning zone.



**Figure 4.** CO content in flue gas is a result of application of individual de-NO<sub>x</sub> methods and their combinations at total fuel input Q = 1.5 m<sup>3</sup>/h and air excess coefficient m = 1.1.

Figure 5 explains the reaction mechanisms leading to NO<sub>x</sub> and CO formation in individual temperature zones of the furnace and allows monitoring of temperature trends resulting from primary de-NO<sub>x</sub> methods application.



**Figure 5.** Measured flue-gas temperatures through the furnace during experiments involving fuel input Q = 1.5 m<sup>3</sup>/h and air excess coefficient m = 1.1.

NO<sub>x</sub> generated in the main combustion zone (Figures 1 and 5, between T13–T14) reacted with fuel remnants injected into the reburn zone (Figures 1 and 5, between T3–T4), which reduced it to molecular nitrogen. Reburning chemistry involves fuel radicals, which reduce NO to N<sub>2</sub> [32,46]. Reburning increases the flue-gas temperature from thermocouple T4 onwards, compared to OFA application or no de-NO<sub>x</sub>-method use.

The addition of overfire air completed combustion in the burn-out zone (Figures 1 and 5, between T4–T5), but the reaction heat released by CO and hydrocarbon fragments was not enough to compensate for the cold, fresh air introduced, and as a result the flue-gas temperature decreased from T5 onwards, compared to the application of reburning alone.

A similar series of measurements was conducted at natural gas thermal input  $Q = 1.8 \text{ m}^3/\text{h}$  and air excess coefficient  $m = 1.2$ , with the results shown in Figures 6 and 7. A comparison of the data shown in Figures 2 and 6 revealed that the latter combustor operation conditions generally yielded higher  $\text{NO}_x$  emissions by around 75 to 100%, which is in accordance with current knowledge on nitrogen oxide formation in combustion processes. Considering the previous finding about FGR application effects, this method was combined with modest reburning (reburning ratio of 10%) and overfire air. Figure 6 documents that the combination of 10% reburning ratio, overfire air, and 10% FGR more than halved the  $\text{NO}_x$  emissions compared to the situation without any primary de- $\text{NO}_x$  method application. Further increases in denitrification efficiency can be followed in Figure 7 with increasing FGR, with the highest efficiency value of over 70% being reached at 20% FGR. In contrast to this, application of either modest reburning (reburning ratio of 10%) or overfire air or their combination did not lead to significant denitrification, and the same could be observed at a lower burner load and lower air excess coefficient—see Figure 2. In both situations the denitrification efficiencies reached below or around 20% maximally.

As Figure 6 further shows, denitrification efficiency is closely coupled with combustion temperature. The decrease in combustion temperature resulting from the application of primary denitrification methods hinders the formation of thermal  $\text{NO}_x$ , which, together with the creation of a reductive environment, leads to effective nitrogen oxide emissions reduction. Test experiments aimed at verification of both temperature measurements' stability and sensitivity to combustion conditions were performed and their results, shown in Appendix C, prove that temperature changes of around  $10 \text{ }^\circ\text{C}$  and higher can be clearly recognized and attributed to process condition changes. This justifies the conclusions drawn from the analysis of the temperature data and their trends presented in Figures 5 and 6.

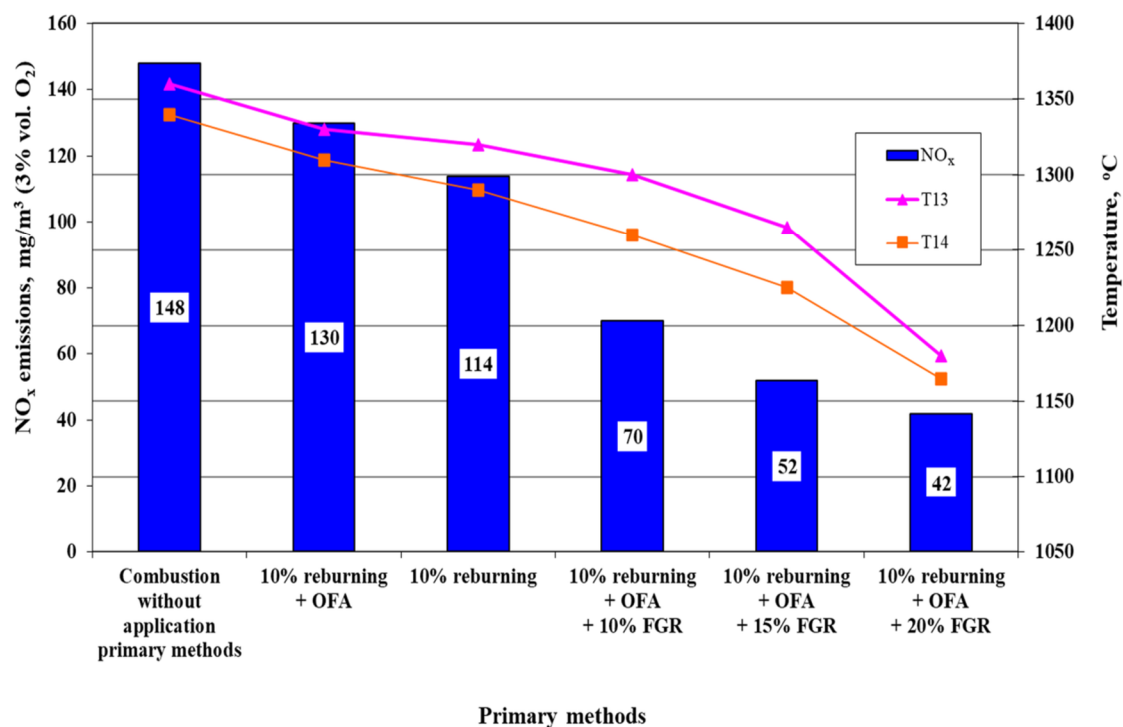


**Figure 6.**  $\text{NO}_x$  emissions (expressed in  $\text{mg}/\text{m}^3$  at 3% vol. oxygen in dry flue gas under normal temperature and pressure) and measured temperatures in the combustion chamber after the application of primary methods in combination at total fuel input  $Q = 1.8 \text{ m}^3/\text{h}$  and air excess coefficient  $m = 1.2$ .

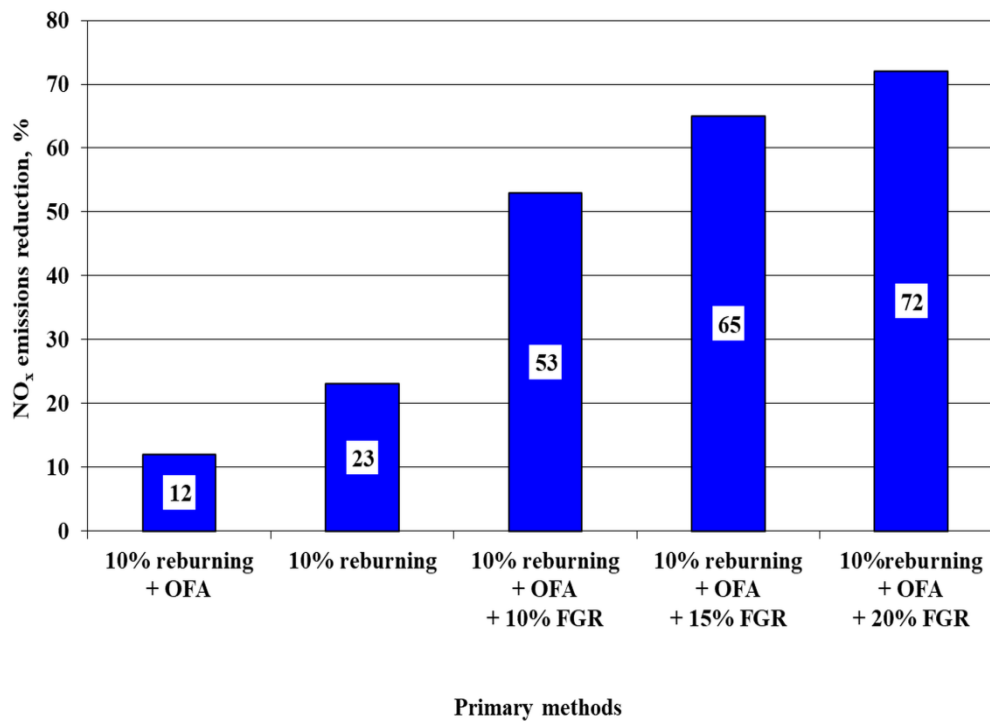


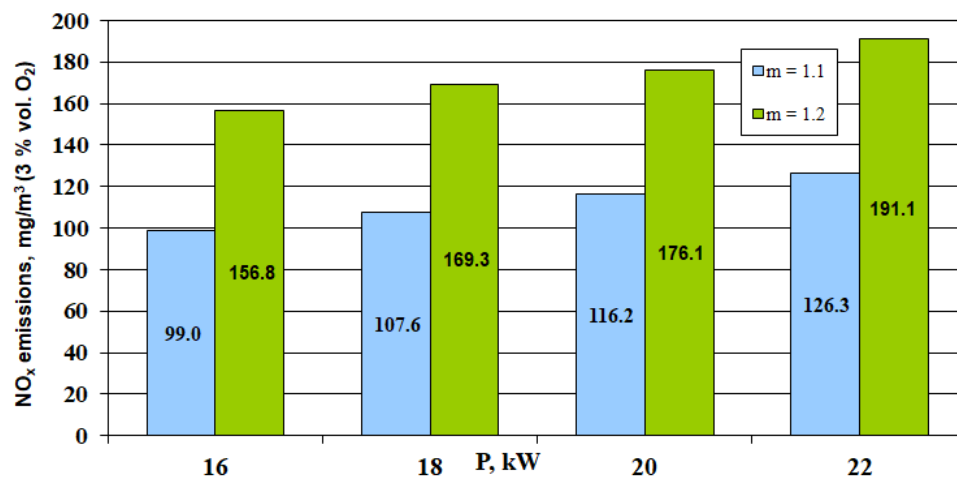
**Figure 7.** NO<sub>x</sub> emissions reduction achieved after application of primary methods and their combinations at total fuel input  $Q = 1.8 \text{ m}^3/\text{h}$  and air excess coefficient  $m = 1.2$ .

It can be concluded that OFA application should be part of any combined primary de-NO<sub>x</sub> method, as it is able to reduce both NO<sub>x</sub> and CO contents in flue gas on its own, and when applied together with reburning and OFA it should ensure very efficient denitrification while still meeting the CO emission limits.

### 3.2. Propane–Butane Gas (PBG) Combustion Experiments

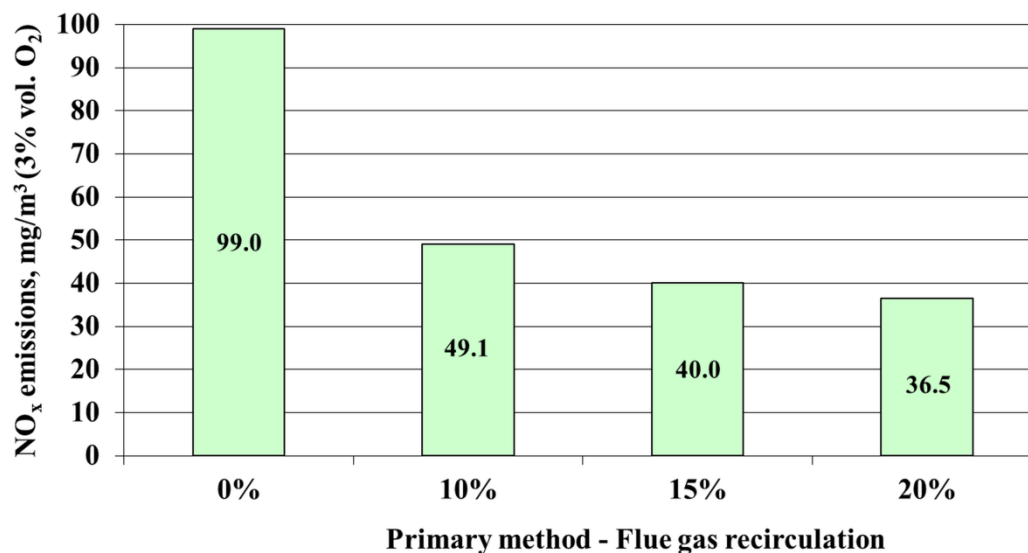
This section presents the results of primary de-NO<sub>x</sub> methods application during propane–butane gas combustion, carried out in parallel with our natural gas combustion experiments. The combustion conditions involved a range of total fuel input  $Q = 16$  to  $22 \text{ kW}$  and overall air excess coefficient  $m = 1.1$  and  $1.2$ , respectively. Having found that flue-gas recirculation was the most efficient denitrification method in natural gas combustion experiments, it was applied as the sole de-NO<sub>x</sub> method in our PBG experiments as well.

Figure 8 provides a comparison of NO<sub>x</sub> emissions in PBG experiments as a result of different fuel input and air excess coefficient values, with no other denitrification method applied. As expected, and in line with our NG experiment results, increased fuel input and air excess coefficient led to an increase in emissions. Nitrogen oxide emissions values in our PBG experiments were around 20% higher than those observed in the NG experiments under identical conditions (i.e.,  $Q = 1.5 \text{ m}^3/\text{h}$  and  $m = 1.1$ ;  $Q = 1.8 \text{ m}^3/\text{h}$  and  $m = 1.2$ ): compare Figures 2 and 6.



**Figure 8.** Nitrogen oxide formation (expressed in  $\text{mg}/\text{m}^3$  at 3% vol. oxygen in dry flue gas under normal temperature and pressure) as a result of variable burner fuel input and air excess coefficient  $m = 1.1$  and 1.2.

The impact of FGR application on  $\text{NO}_x$  emissions reduction in PGB experiments at burner power input 16 kW and air excess coefficient  $m = 1.1$  is shown in Figure 9. The obtained results are similar to those in our NG experiments, yielding an  $\text{NO}_x$  content decrease with the introduction and increased share of flue-gas recirculation. Both Figures 3 and 9 reveal that the application of 10% FGR decreased the  $\text{NO}_x$  emissions approximately by half, and a further emissions reduction was achieved with greater FGR increase. Denitrification efficiency of almost 65% was achieved at 20% FGR in our PGB experiments, which is somewhat lower than the almost 75% efficiency documented in the NG experiments under identical conditions.



**Figure 9.**  $\text{NO}_x$  emissions (expressed in  $\text{mg}/\text{m}^3$  at 3% vol. oxygen in dry flue gas under normal temperature and pressure) dependence on flue-gas recirculation at burner power input 16 kW and air excess coefficient  $m = 1.1$ .

Similar to the NG experiments, denitrification was found to be closely related to flue-gas temperature in the PGB combustion chamber. Its values for 10%, 15%, and 20% FGR are provided in Figure 10. The more modest decrease in combustion temperature (thermocouples T13 and T14) of around 50 °C documented in Figure 10 resulting from an FGR increase from 10% to 20% is lower than

the over 100 °C combustion temperature decrease shown in Figure 6 resulting from FGR increase in the same range in the NG experiments. This probably allows for a partial explanation of why the denitrification efficiency increase in our PBG experiments in the range of 10% to 20% FGR is lower than in the NG experiments.

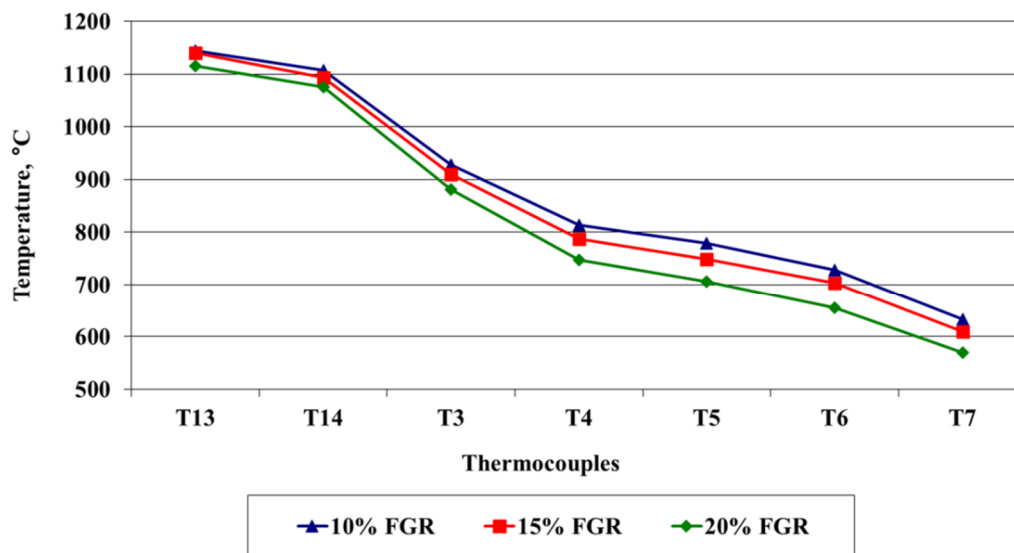


**Figure 10.** Effect of increasing flue-gas recirculation share on the course of the temperature field through the furnace at burner power input 16 kW and air excess coefficient  $m = 1.1$ .

For this reason, experiments with FGR application alone during both NG and PBG combustion are compared in Figure 11 in terms of calculated  $\text{NO}_x$  emissions reduction efficiency.

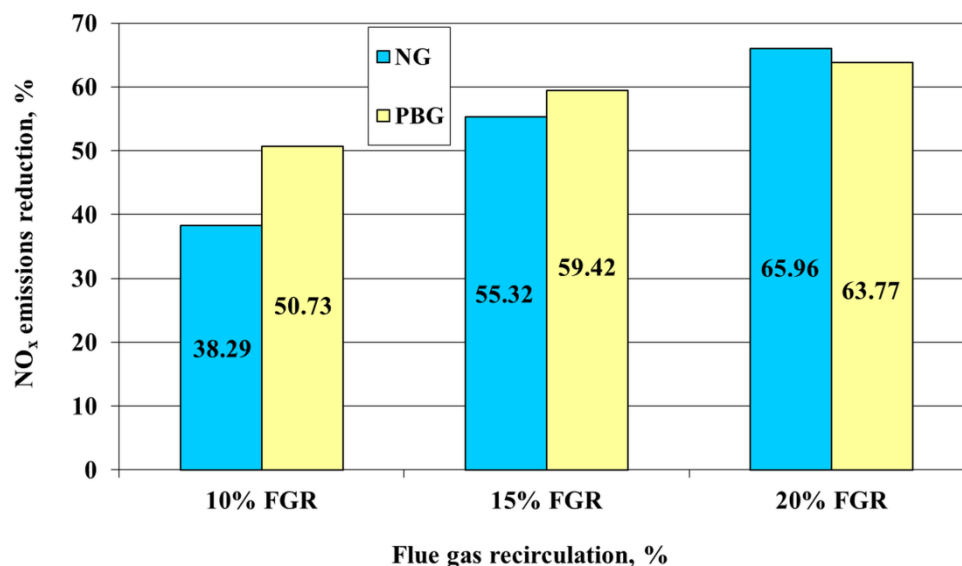


**Figure 11.** Nitrogen oxide emissions reduction after the application of flue-gas recirculation: comparison of natural gas (NG) and propane-butane gas (PBG) combustion at various flue-gas recirculation rates. For both fuels, burner power input was 16 kW and air excess coefficient  $m = 1.1$ .

The trend in nitrogen oxide emissions decrease with increasing FGR can be readily observed in both fuel-type experiments, while the previously commented steeper  $\text{NO}_x$  emissions decrease in NG experiments is clearly confirmed. As a result of the  $\text{NO}_x$  formation reaction mechanisms, the emissions

were suppressed due not only to the lower combustion temperature but also to the lower oxygen partial pressure resulting from FGR implementation. The greater NO<sub>x</sub> emissions reductions observed in our PBG experiments compared to those in the NG experiments most probably resulted from slower combustion of PBG fuel and from its higher volumetric heating value. Higher PBG adiabatic flame temperature compared to NG can play a significant role in this respect too. It results from the observations above that combusted fuel type as well as combustion conditions play an important role in NO<sub>x</sub> formation and reduction processes. Combustion of PBG yields lower volumetric flow of recirculated flue gas compared to NG for the same burner heat input.

#### 4. Discussion

Our experiments conducted with natural gas and PBG fuels allowed us to document several trends regarding nitrogen oxide and carbon monoxide contents in flue gas from a laboratory furnace:

1. Considering de-NO<sub>x</sub> methods applied individually (Figures 2 and 3), FGR yielded the highest denitrification efficiencies of up to 74% (at 20% FGR), followed by reburning (61% at 25% reburning ratio), whereas OFA application resulted only in a modest 21% NO<sub>x</sub> concentration decrease. FGR appears to be the most promising method for decreasing NO<sub>x</sub> emissions, regardless of the type of gaseous fuel combusted (compare Figures 3 and 9). A range of flue-gas denitrification efficiencies due to FGR implementation is reported in the literature, starting with up to 30% or up to 50% in burners equipped with internal flue-gas recirculation systems [38,39] and exceeding this in external recirculation systems [15]. Thus, it can be concluded that external flue-gas recirculation appears to be a more efficient de-NO<sub>x</sub> method, though it requires bigger intervention in boiler or furnace design than the mere implementation of burners with internal recirculation.
2. Combined application of de-NO<sub>x</sub> methods revealed negative synergic effects with OFA + 10% reburning, achieving a lower NO<sub>x</sub> concentration reduction than the application of OFA and 10% reburning individually (Figures 2 and 6). In contrast, the available experimental and numerical studies [14,42] propose the reburning + OFA combination as a very effective means of flue-gas denitrification and report positive synergy effects. Combined application of 10% reburning + OFA + 20% FGR reduced the NO<sub>x</sub> content in flue gas by 72%, which is in line with de-NO<sub>x</sub> efficiencies of over 50% for combined method application reported in the available literature. For comparison, [43] used a combined OFA + FGR method in a 100 kW facility, combusting various gaseous and solid fuels, reaching up to 80% decrease in NO content in flue gas.
3. Increasing the burner load from 16 to 18 kW and the air excess coefficient from 1.1 to 1.2 resulted in 50% to 70% higher NO<sub>x</sub> emissions, regardless of whether NG or PBG was combusted (Figures 2, 6 and 8), with the air excess coefficient increase visibly playing the major role in NO<sub>x</sub> emissions increase, which is in line with the findings of the study by Dutka et al., 2016 [5]. However, denitrification efficiencies of individual methods and their combinations appeared to be only modestly affected by burner load and air excess coefficient in our experiments (Figures 2, 3 and 7).
4. FGR, as the most promising de-NO<sub>x</sub> method, was applied in our PBG combustion tests, achieving similar denitrification efficiency as in the NG combustion tests (Figure 11). However, denitrification efficiency increase with rising flue-gas recirculation was more pronounced in the case of NG combustion. This could be explained in terms of the far more pronounced temperature drop in the main combustion chamber (thermocouples T13, T14) observed in our NG combustion tests with rising flue-gas recirculation. Comparison of the respective temperature values in Figures 6 and 10 reveals that temperature drops of over 100 °C could be documented for NG combustion compared to around only 50 °C for PBG combustion. This finding deserves more attention and further investigation in the future, as the relevant literature surveyed [43] suggests that similar trends should be obtained with similar gaseous reburning fuels.
5. FGR yielded a visible decrease in carbon monoxide emissions (Figure 4). A modest decrease in flue-gas CO content could be seen after OFA application as well; however, reburning produced a

sharp, more than 12-fold increase in these emissions ( $1251 \text{ mg/m}^3$ ) compared to that without any de- $\text{NO}_x$  method application ( $101 \text{ mg/m}^3$ ). This could partly be resolved by combined reburning + OFA application, but the reburning fuel share should be limited to around 15% in order not to violate the CO emissions limit of  $200 \text{ mg/m}^3$ . In contrast to this, [35] did not observe any significant effect of reburning application on CO emissions, despite similar experimental furnace heat input (65 kW vs. 16 to 22 kW in this study) and despite the same fuel being used both as the main and reburning fuel (NG). [44] performed experiments with various recirculated flue-gas introduction spots in an experimental heavy fuel oil-fired furnace, namely direct mixing with primary air, separate introduction after primary air supply, and separate introduction after secondary air supply. Compared to basic-case CO emissions of around  $20 \text{ mg/m}^3$ , all reburning options produced an increase in CO emissions, compared to operation without FGR. The differences documented above allow us to conclude that CO formation and conversion to  $\text{CO}_2$  with primary de- $\text{NO}_x$  methods application is a complex phenomenon yielding very variable results even under seemingly similar experimental conditions. Further work on this topic needs to be done.

## 5. Conclusions

An experimental laboratory furnace setup was used to assess the trends and variations in nitrogen oxide and carbon monoxide emissions from natural gas and propane–butane gas combustion. Individual primary flue-gas denitrification methods as well as their combined use allowed us to identify the most efficient individual method (flue-gas recirculation) and the most efficient combination of methods (overfire air + reburning + flue-gas recirculation). The achieved denitrification efficiencies (close to 65% for propane–butane gas combustion or even over 70% for natural gas combustion) are promising and suggest that further research should be aimed at investigating the use of wood gasification gas as fuel in the test rig. Combined application of 10% reburning + OFA + 20% FGR reduced the flue gas'  $\text{NO}_x$  content by 72% in the studied furnace under the given combustion conditions. Considering the given conditions, the fuels combusted, and the furnace geometry, this combination can be recommended as the most efficient one for flue-gas denitrification.

Our carbon monoxide emissions results practically ruled out the application of reburning in the experimental setup, and this became even worse when CO-rich gas was combusted instead of natural gas. Flue-gas recirculation appears to be the most viable method that can readily be applied to different combustion designs and fuels used, as it exhibits both significant de- $\text{NO}_x$  and de-CO efficiency, although its application limits should be subject to more focused study.

**Author Contributions:** Conceptualization, L.L. and J.K.; methodology, L.L. and J.K.; validation, M.F. and G.J.; investigation, L.L. and P.L.; resources, M.R.; data curation, L.L. and J.J.; writing—original draft preparation, L.L., M.V., and G.J.; writing—review and editing, M.V., J.J., and P.L.; visualization, P.L.; supervision, G.J.; funding acquisition, L.L., M.R., and M.F. All authors have read and agreed to the published version of the manuscript.

**Funding:** This work was financially supported by the Slovak Research and Development Agency, Grants No. APVV-16-0192 and APVV-18-0134 and by the Slovak Scientific Agency, Grant No. VEGA 1/0691/18.

**Conflicts of Interest:** The authors declare no conflict of interest. The funders had no role in the design of the study; in the collection, analyses, or interpretation of data; in the writing of the manuscript, or in the decision to publish the results.

## List of Symbols and Abbreviations

|               |                          |
|---------------|--------------------------|
| A             | analyzer                 |
| FGR           | flue-gas recirculation   |
| LNB           | low $\text{NO}_x$ burner |
| m             | air excess coefficient   |
| NG            | natural gas              |
| $\text{NO}_x$ | nitrogen oxides          |
| OFA           | overfire air             |

|                   |   |                   |
|-------------------|---|-------------------|
| PBG               | propane–butane gas  |                   |
| Pt                | thermal power input   | kW                |
| p                 | pressure  | Pa                |
| Q                 | volumetric flow   | m <sup>3</sup> /h |
| T                 | temperature   | °C                |
| V                 | throttle valve  |                   |
| R                 | emissions reduction   | (%)               |
| C <sub>WAPM</sub> | nitrogen oxide emissions without application of primary methods |                   |
| C <sub>APM</sub>  | nitrogen oxides emissions with application of primary methods   |                   |
| max               | maximum   |                   |
| min               | minimum   |                   |
| stat              | static (pressure)   |                   |
| total             | total (pressure)  |                   |

## Appendix A

Tables A1 and A2 provide information about the NO<sub>x</sub> and CO measurement method for the Testo 350 analyzer (A2 analyzer) as stated by the manufacturer [47]. Likewise, Table A3 shows information relating to the Testo 325 (A3 analyzer) measurement method and error range as stated by the manufacturer [48].

**Table A1.** Nitrogen oxide measurement method and measurement error range stated by Testo 350 analyzer series manufacturer [47].

| Testo 350 M and Testo 350 XL |                        |                        |                        |                       |
|------------------------------|------------------------|------------------------|------------------------|-----------------------|
|                              | NO                     |                        | NO <sub>2</sub>        |                       |
| Measurement method           | Electrochemical sensor |                        | Electrochemical sensor |                       |
| Metering range               | 0 to 3000 ppm          |                        | 0 to 500 ppm           |                       |
| Measurement error range      | 0 to 99.9 ppm          | ±5 ppm                 | 0 to 99.9 ppm          | ±5 ppm                |
|                              | 100 to 1999.9 ppm      | ±5% of measured value  | 100 to 500 ppm         | ±5% of measured value |
|                              | 2000 to 3000 ppm       | ±10% of measured value |                        | -                     |
| Depiction accuracy           | 1 ppm                  |                        | 0.1 ppm                |                       |

**Table A2.** Carbon monoxide measurement method and measurement error range stated by Testo 350 analyzer series manufacturer [47].

| Testo 350 M and Testo 350 XL |                        |                        |
|------------------------------|------------------------|------------------------|
|                              | CO                     |                        |
| Measurement method           | Electrochemical sensor |                        |
| Metering range               | 0 to 10,000 ppm        |                        |
| Measurement error range      | 0 to 199 ppm           | ±10 ppm                |
|                              | 200 to 2000 ppm        | ±5% of measured value  |
|                              | 2001 to 10,000 ppm     | ±10% of measured value |
| Depiction accuracy           | 1 ppm                  |                        |

**Table A3.** Measurement method and measurement error range stated by Testo 325-I analyzer manufacturer [48].

| Testo 325-I             |                        |                        |                        |                        |
|-------------------------|------------------------|------------------------|------------------------|------------------------|
|                         | NO                     |                        | CO                     |                        |
| Measurement method      | Electrochemical sensor |                        | Electrochemical sensor |                        |
| Metering range          | 0–1000 ppm             |                        | 0–2000 ppm             |                        |
| Measurement error range | 0 to 400 ppm           | <20 ppm                | 0 to 400 ppm           | <20 ppm                |
|                         | >200 ppm               | <±5% of measured value | >400 ppm               | <±5% of measured value |
|                         |                        |                        |                        |                        |
| Depiction accuracy      | 1 ppm                  |                        | 1 ppm                  |                        |

## Appendix B

After primary burner ignition, the desired fuel volumetric flow and air excess coefficient were set for combustion without any primary denitrification method application. Afterwards, stable combustion conditions, a stable temperature profile, and stable oxygen concentration in the flue gas were reached, which took, depending on initial conditions, up to several hours. On reaching the stationary state, values of NO, NO<sub>2</sub>, O<sub>2</sub>, and CO concentrations measured by the analyzers and temperatures indicated by all thermocouples were recorded pointwise at five-minute intervals. Temperature readings were continuously recorded by the Comet data unit.

After all process parameter readings were done, additional air was introduced in the OFA zone (see Figure 1) so as to reach a constant final air excess coefficient ( $m = 1.1$  or  $1.2$ ) in the place where analyzer A2 was located. After reaching stationary conditions (see the previous paragraph), readings of gas concentrations and temperatures were recorded periodically within 30 to 45 min of stable furnace operation at five-minute intervals.

In the FGR experiments, the evaluated process parameters included the amount of recirculated flue gas (10 to 20%), air excess coefficient, combustion temperature, and fuel volumetric flow. Various fuel volumetric flows were used in the experiments. The recirculation rate was estimated from the oxygen material balance setup using the data on the oxygen concentration (Analyzers A1,2) and on fuel and combustion air volumetric flows. Starting with zero FGR, flue-gas recirculation was introduced until the desired oxygen content in the air–flue gas mixture was reached. It was kept constant during the given measurement, which ensured a constant flue-gas recirculation rate. Flue-gas recirculation rate was increased afterwards until a new value of oxygen content in the air–flue gas mixture was reached, and the measurement was repeated.

When using the reburning method, the reburning fuel was introduced in the middle part of the flue-gas duct (see Figure 1) with its amount ranging between 10 to 25% of total fuel combusted (the sum of primary and reburning fuel), while the amount of total fuel combusted was kept constant.

Nitrogen oxide and carbon monoxide values shown and discussed in the manuscript are average concentration values obtained from individual measurements for the given fuel consumption and air excess coefficient.

## Appendix C

Figures A1 and A2 show the time courses of measured temperature values in the furnace during test experiments. Test experiments were aimed at verifying sufficient stability of temperature measurements during stable furnace operation as well as their sufficient sensitivity to the changes of combustion conditions.

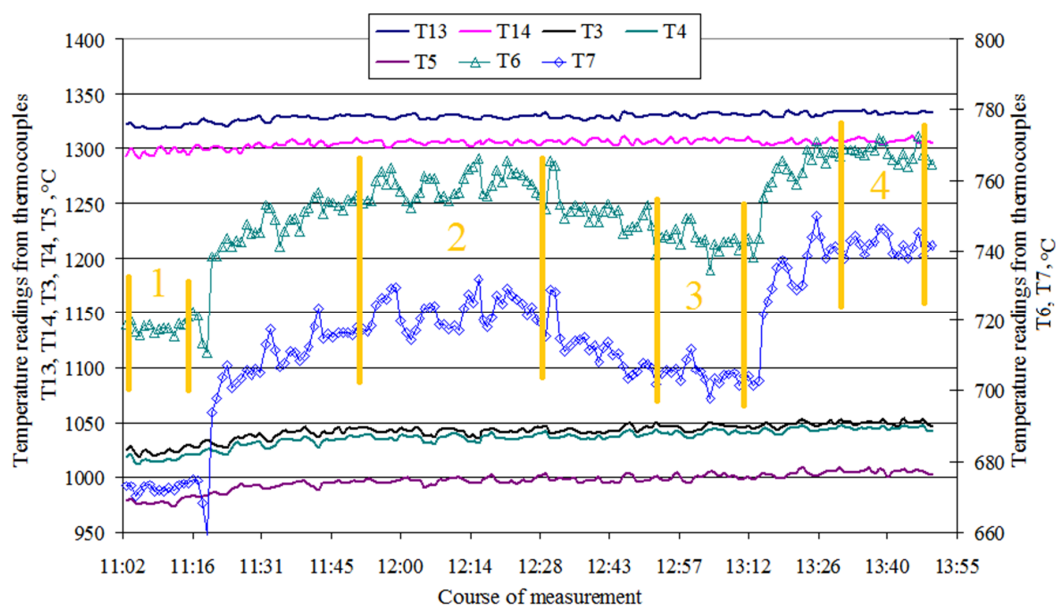


**Figure A1.** Measured flue-gas temperatures through the furnace during test experiments involving fuel input  $Q = 1.6 \text{ m}^3/\text{h}^1$  and air excess coefficient  $m = 1.1$  with varying reburning ratio. Stable operation states as indicated in the Figure: 1 = without any primary method applied; 2 = reburning share of 25%; 3 = reburning share of 20%; 4 = reburning share of 35%.

As can be recognized from both Figures A1 and A2, temperatures measured by individual thermocouples vary within a few °C during steady operation of the furnace. Contrary to that, changes of temperatures measured by thermocouples T6 and T7, resulting from performed step changes of reburning share, are clearly recognizable. Moreover, well-defined individual temperature plateaus corresponding to stable operation of the furnace with

different reburning shares can be seen as well. The results of preliminary experiments proved that the temperature measurements were both sufficiently stable and sensitive to the changes of the operation conditions.

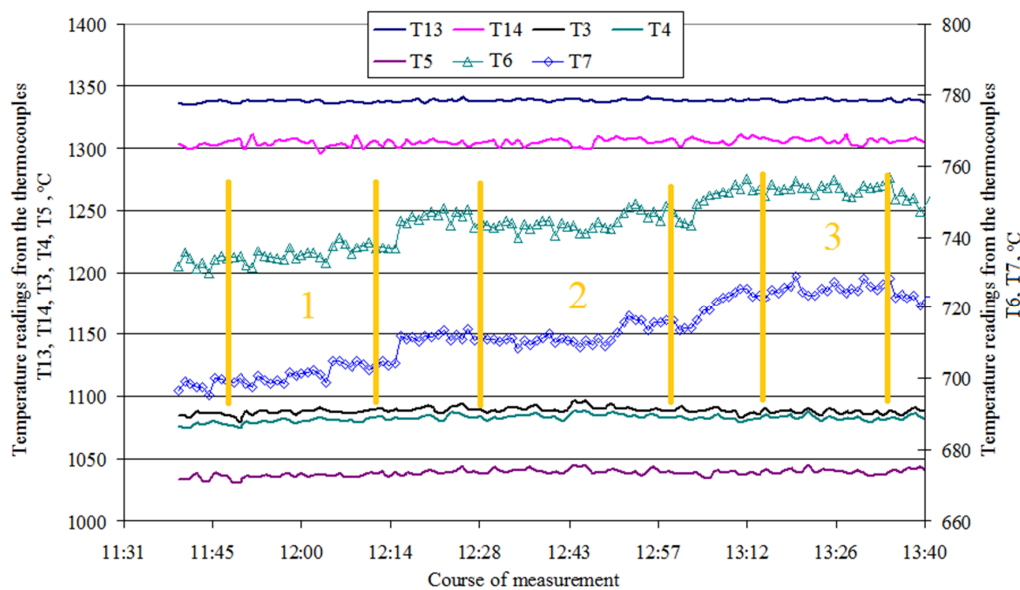


**Figure A2.** Measured flue-gas temperatures through the furnace during test experiments involving fuel input  $Q = 1.8 \text{ m}^3/\text{h}$  and air excess coefficient  $m = 1.1$  with varying reburning ratio. Stable operation states as indicated in the Figure: 1 = reburning share of 20%; 2 = reburning share of 25%; 3 = reburning share of 35%.

## References

- Munawar, M.E. Human health and environmental impacts of coal combustion and post-combustion wastes. *J. Sustain. Min.* **2018**, *17*, 87–96. [[CrossRef](#)]
- Lin, F.; Wang, Z.; Zhang, Z.; He, Y.; Zhu, Y.; Shao, J.; Yuan, D.; Chen, G.; Cen, K. Flue gas treatment with ozone oxidation: An overview on NO, organic pollutants, and mercury. *Chem. Eng. J.* **2020**, *382*, 123030. [[CrossRef](#)]
- Mohan, S.; Dinesha, P.; Kumar, P. NO<sub>x</sub> reduction behaviour in copper zeolite catalysts for ammonia SCR systems: A review. *Chem. Eng. J.* **2020**, *384*, 123253. [[CrossRef](#)]
- Gholami, F.; Tomas, M.; Gholami, Z.; Vakili, M. Technologies for the nitrogen oxides reduction from flue gas: A review. *Sci. Total Environ.* **2020**, *714*, 136712. [[CrossRef](#)] [[PubMed](#)]
- Dutka, M.; Ditaranto, M.; Løvås, T. NO<sub>x</sub> emissions and turbulent flow field in a partially premixed bluff body burner with CH<sub>4</sub> and H<sub>2</sub> fuels. *Int. J. Hydrog. Energy* **2016**, *41*, 12397–12410. [[CrossRef](#)]
- Arun, S.; Raghuram, S.; Sreenivasan, R.; Raghavan, V. Effect of hydrogen addition in the co-flow of a methane diffusion flame in reducing nitric oxide emissions. *Int. J. Hydrog. Energy* **2012**, *37*, 19198–19209. [[CrossRef](#)]
- Bělohradský, P.; Skryja, P.; Hudák, I. Experimental study on the influence of oxygen content in the combustion air on the combustion characteristics. *Energy* **2014**, *75*, 116–126. [[CrossRef](#)]
- Habib, M.A.; Elshafei, M.; Dajani, M. Influence of combustion parameters on NO<sub>x</sub> production in an industrial boiler. *Comput. Fluids* **2008**, *37*, 12–23. [[CrossRef](#)]
- Liu, Y.; Zhang, X.; Ding, J. Chemical effect of NO on CH<sub>4</sub> oxidation during combustion in O<sub>2</sub>/NO environments. *Chem. Phys. Lett.* **2019**, *727*, 59–65. [[CrossRef](#)]
- Cozzi, F.; Coghe, A. Effect of air staging on a coaxial swirled natural gas flame. *Exp. Therm. Fluid Sci.* **2012**, *43*, 32–39. [[CrossRef](#)]
- Fan, W.; Chen, J.; Feng, Z.; Wu, X.; Liu, S. Effects of reburning fuel characteristics on NO<sub>x</sub> emission during pulverized coal combustion and comparison with air-staged combustion. *Fuel* **2020**, *265*, 117007. [[CrossRef](#)]
- Smoot, L.D.; Hill, S.C.; Xu, H. NO<sub>x</sub> control through reburning. *Prog. Energy Combust. Sci.* **1998**, *24*, 385–408. [[CrossRef](#)]

13. Chen, S.; Xing, Y.; Li, A. CFD investigation on Low-NO<sub>x</sub> strategy of folded flame pattern based on fuel-staging natural gas burner. *Appl. Therm. Eng.* **2017**, *112*, 1487–1496. [[CrossRef](#)]
14. Motyl, P.; Lach, J. Computational Modelling of Retrofitting a Coal Fired Boiler Type OP-230 for Predicting NO<sub>x</sub> Reduction. *J. Therm. Sci.* **2018**, *27*, 433–439. [[CrossRef](#)]
15. Gamrat, S.; Poraj, J.; Bodys, J.; Smolka, J.; Adamczyk, W. Influence of external flue gas recirculation on gas combustion in a coke oven heating system. *Fuel Process. Technol.* **2016**, *152*, 430–437. [[CrossRef](#)]
16. Pawlak-Kruczek, H.; Ostrycharczyk, M.; Czerep, M.; Baranowski, M.; Zgóra, J. Examinations of the process of hard coal and biomass blend combustion in OEA (oxygen enriched atmosphere). *Energy* **2015**, *92*, 40–46. [[CrossRef](#)]
17. Duan, L.; Duan, Y.; Zhao, C.; Anthony, E.J. NO emission during co-firing coal and biomass in an oxy-fuel circulating fluidized bed combustor. *Fuel* **2015**, *150*, 8–13. [[CrossRef](#)]
18. Varol, M.; Symonds, R.; Anthony, E.J.; Lu, D.; Jia, L.; Tan, Y. Emissions from co-firing lignite and biomass in an oxy-fired CFBC. *Fuel Process. Technol.* **2018**, *173*, 126–133. [[CrossRef](#)]
19. Liu, Q.; Shi, Y.; Zhong, W.; Yu, A. Co-firing of coal and biomass in oxy-fuel fluidized bed for CO<sub>2</sub> capture: A review of recent advances. *Chin. J. Chem. Eng.* **2019**, *27*, 2261–2272. [[CrossRef](#)]
20. Šlančiauskas, A.; Striūgas, N. Various compositions of burner gas fuel and air streams for lower CO and NO<sub>x</sub> yield. *Int. J. Heat Mass Transf.* **2012**, *55*, 5609–5615. [[CrossRef](#)]
21. Korpela, T.; Kumpulainen, P.; Majanne, Y.; Häyrinen, A.; Lautala, P. Indirect NO<sub>x</sub> emissions monitoring in natural gas fired boilers. *Control Eng. Pract.* **2017**, *65*, 11–25. [[CrossRef](#)]
22. Bilbao, R.; Alzueta, M.U.; Millera, A.; Cantín, V. Experimental study and modelling of the burnout zone in the natural gas reburning process. *Chem. Eng. Sci.* **1995**, *50*, 2579–2587. [[CrossRef](#)]
23. Lukáč, L.; Suchý, T.; Doliňáková, A. Analýza vplyvu aplikácie primárnych metód na znižovanie emisií NO<sub>x</sub>. (Analysis of primary methods application influence on NO<sub>x</sub> emissions lowering; in Slovak). *Acta Metall. Slovaca* **2005**, *11*, 199–204.
24. Elbaz, A.M.; Moneib, H.A.; Shebil, K.M.; Roberts, W.L. Low NO<sub>x</sub>—LPG staged combustion double swirl flames. *Renew. Energy* **2019**, *138*, 303–315. [[CrossRef](#)]
25. Hesselmann, G.J. Optimization of combustion by fuel testing in a NO<sub>x</sub> reduction test facility. *Fuel* **1997**, *76*, 1269–1275. [[CrossRef](#)]
26. Lukáč, L.; Holoubek, D. Využitie primárnych deNO<sub>x</sub> metód v uhoľných kotloch. (Use of primary deNO<sub>x</sub> methods in coal boilers; in Slovak). *Acta Metall. Slovaca* **2002**, *8*, 109–117.
27. Sung, Y.; Lee, S.; Kim, C.; Jun, D.; Moon, C.; Choi, G.; Kim, D. Synergistic effect of co-firing woody biomass with coal on NO<sub>x</sub> reduction and burnout during air-staged combustion. *Exp. Therm. Fluid Sci.* **2016**, *71*, 114–125. [[CrossRef](#)]
28. Liang, Z.; Chen, H.; Zhao, B.; Jia, J.; Cheng, K. Synergetic effects of firing gases/coal blends and adopting deep air staging on combustion characteristics. *Appl. Energy* **2018**, *228*, 499–511. [[CrossRef](#)]
29. Bilbao, R.; Millera, A.; Alzueta, M.U.; Prada, L. Evaluation of the use of different hydrocarbon fuels for gas reburning. *Fuel* **1997**, *76*, 1401–1407. [[CrossRef](#)]
30. Harding, N.S.; Adams, B.R. Biomass as a reburning fuel: A specialized cofiring application. *Biomass Bioenergy* **2000**, *19*, 429–445. [[CrossRef](#)]
31. Kicherer, A.; Spliethoff, H.; Maier, H.; Hein, K.R.G. The effect of different reburning fuels on NO<sub>x</sub> reduction. *Fuel* **1994**, *73*, 1443–1446. [[CrossRef](#)]
32. Smart, J.P.; Morgan, D.J. The effectiveness of multi-fuel reburning in an internally fuel-staged burner for NO<sub>x</sub> reduction. *Fuel* **1994**, *73*, 1437–1442. [[CrossRef](#)]
33. Su, S.; Xiang, J.; Sun, L.; Hu, S.; Zhang, Z.; Zhu, J. Application of gaseous fuel reburning for controlling nitric oxide emissions in boilers. *Fuel Process. Technol.* **2009**, *90*, 396–402. [[CrossRef](#)]
34. Casaca, C.; Costa, M. Detailed measurements in a laboratory furnace with reburning. *Fuel* **2011**, *90*, 1090–1100. [[CrossRef](#)]
35. Chae, T.; Lee, J.; Yang, W.; Ryu, C. Characteristics of syngas reburning in a natural gas firing furnace—Effects of combustible gas species in the syngas. *J. Mech. Sci. Technol.* **2016**, *30*, 3861–3868. [[CrossRef](#)]
36. Zhou, A.; Xu, H.; Xu, M.; Yu, W.; Li, Z.; Yang, W. Numerical investigation of biomass co-combustion with methane for NO<sub>x</sub> reduction. *Energy* **2020**, *194*, 116868. [[CrossRef](#)]
37. Holoubek, D. *Spaľovacie Zariadenia, Výmenníky Tepla a Kotly. (Combustion Appliances, Heat Exchangers and Boilers; in Slovak)*; TU v Košiciach: Košice, Slovakia, 2002; p. 215, ISBN 80-7099-832-6.

38. Delabroy, O.; Haile, E.; Lacas, F.; Candel, S.; Pollard, A.; Sobiesiak, A.; Becker, H.A. Passive and active control of NO<sub>x</sub> in industrial burners. *Exp. Therm. Fluid Sci.* **1998**, *16*, 64–75. [[CrossRef](#)]
39. Shi, B.; Hu, J.; Peng, H.; Ishizuka, S. Effects of internal flue gas recirculation rate on the NO emission in a methane/air premixed flame. *Combust. Flame* **2018**, *188*, 199–211. [[CrossRef](#)]
40. Shalaj, V.V.; Mikhajlov, A.G.; Novikova, E.E.; Terebilov, S.V.; Novikova, T.V. Gas Recirculation Impact on the Nitrogen Oxides Formation in the Boiler Furnace. *Procedia Eng.* **2016**, *152*, 434–438. [[CrossRef](#)]
41. Shalaj, V.V.; Mikhailov, A.G.; Slobodina, E.N.; Terebilov, S.V. Issues on Nitrogen Oxides Concentration Reduction in the Combustion Products of Natural Gas. *Procedia Eng.* **2015**, *113*, 287–291. [[CrossRef](#)]
42. Hodžić, N.; Kazagić, A.; Smajević, I. Influence of multiple air staging and reburning on NO<sub>x</sub> emissions during co-firing of low rank brown coal with woody biomass and natural gas. *Appl. Energy* **2016**, *168*, 38–47. [[CrossRef](#)]
43. Normann, F.; Andersson, K.; Johnsson, F.; Leckner, B. NO<sub>x</sub> reburning in oxy-fuel combustion: A comparison between solid and gaseous fuels. *Int. J. Greenh. Gas Control* **2011**, *5*, 120–126. [[CrossRef](#)]
44. Ling, Z.; Zhou, H.; Ren, T. Effect of the flue gas recirculation supply location on the heavy oil combustion and NO<sub>x</sub> emission characteristics within a pilot furnace fired by a swirl burner. *Energy* **2015**, *91*, 110–116. [[CrossRef](#)]
45. Lipardi, A.C.A.; Versailles, P.; Watson, G.M.G.; Bourque, G.; Bergthorson, J.M. Experimental and numerical study on NO<sub>x</sub> formation in CH<sub>4</sub>-air mixtures diluted with exhaust gas components. *Combust. Flame* **2017**, *179*, 325–337. [[CrossRef](#)]
46. Glarborg, F.; Miller, J.A.; Ruscic, B.; Klippenstein, S.J. Modeling nitrogen chemistry in combustion. *Prog. Energy Combust. Sci.* **2018**, *67*, 31–68. [[CrossRef](#)]
47. Instruction Manual for the Testo 350M-XL Analyzers, Page 11. Available online: [http://ktest.sk/testo2006/Emissions\\_service\\_thermal/testo\\_350M-XL.pdf](http://ktest.sk/testo2006/Emissions_service_thermal/testo_350M-XL.pdf) (accessed on 17 July 2020).
48. Instruction Manual for the Testo 325-I Analyzer, Page 8. Available online: <https://static-int.testo.com/media/ee/39/e503b6bedf0c/testo-325-1-2-sira-Instruction-Manual.pdf> (accessed on 17 July 2020).



© 2020 by the authors. Licensee MDPI, Basel, Switzerland. This article is an open access article distributed under the terms and conditions of the Creative Commons Attribution (CC BY) license (<http://creativecommons.org/licenses/by/4.0/>).